REGION-BASED 3D SURFACE RECONSTRUCTION USING IMAGES ACQUIRED BY LOW-COST UNMANNED AERIAL SYSTEMS

Z. Lari [a]*, A. Al-Rawabdeh [a], F. He [b], A. Habib [b], N. El-Sheimy [a]

[a] Department of Geomatics Engineering, University of Calgary, 2500 University Dr. NW, Calgary, Canada
(zlari, amalrawa, el-sheimy)@ucalgary.ca
[b] Lyles School of Civil Engineering, Purdue University, 550 Stadium Mall Drive, West Lafayette, IN, USA 47907
(he270, ahabib)@purdue.edu

KEY WORDS: Reconstruction, Unmanned Aerial Systems (UAS), Semi-Global dense Matching (SGM), Segmentation, Texturing

ABSTRACT:

Accurate 3D surface reconstruction of our environment has become essential for an unlimited number of emerging applications. In the past few years, Unmanned Aerial Systems (UAS) are evolving as low-cost and flexible platforms for geospatial data collection that could meet the needs of aforementioned application and overcome limitations of traditional airborne and terrestrial mobile mapping systems. Due to their payload restrictions, these systems usually include consumer-grade imaging and positioning sensor which will negatively impact the quality of the collected geospatial data and reconstructed surfaces. Therefore, new surface reconstruction surfaces are needed to mitigate the impact of using low-cost sensors on the final products. To date, different approaches have been proposed to for 3D surface construction using overlapping images collected by imaging sensor mounted on moving platforms. In these approaches, 3D surfaces are mainly reconstructed based on dense matching techniques. However, generated 3D point clouds might not accurately represent the scanned surfaces due to point density variations and edge preservation problems. In order to resolve these problems, a new region-based 3D surface renostruction trchnique is introduced in this paper. This approach aims to generate a 3D photo-realistic model of individually scanned surfaces within the captured images. This approach is initiated by a Semi-Global dense Matching procedure is carried out to generate a 3D point cloud from the scanned area within the collected images. The generated point cloud is then segmented to extract individual planar surfaces. Finally, a novel region-based texturing technique is implemented for photorealistic reconstruction of the extracted planar surfaces. Experimental results using images collected by a camera mounted on a low-cost UAS demonstrate the feasibility of the proposed approach for photorealistic 3D surface reconstruction.

1. INTRODUCTION

In recent years, there has been a growing demand for accurate 3D surface reconstruction for different applications such as urban planning, environmental monitoring, cultural heritage documentation, structural health monitoring, landslide hazard analysis, and localization. The needs of these emerging applications cannot be satisfied by traditional mapping due to the limitations in financial and technical resources. Recent advances in hardware (low-cost digital imaging and navigation systems) and software development have made it possible to accurately reconstruct 3D surfaces without using costly mapping-grade data acquisition systems. Moreover, advancements in mobile mapping systems (airborne and terrestrial) have made accurate 3D surface reconstruction more feasible whenever and wherever required (El-Sheimy, 2005; Tao and Li, 2007). However, these systems are quite expensive and cannot be rapidly and efficiently deployed. Hence, Unmanned Aerial Vehicles (UAVs) are evolving as new platforms that could meet the needs of different applications and overcome the limitations of the aforementioned mapping systems (Eisenbeiss, 2011; Everaerts, 2008). The characteristics of these systems – e.g., flexibility, low-cost deployment, flying in lower elevation and higher speed – make them an optimal platform for emerging mapping, modelling, and monitoring applications (Nagai et al., 2009).

In low-cost UAV systems, payload restriction enforces using consumer-grade imaging sensors (usually cameras) which will negatively affect the quality of the reconstructed surfaces using the images acquired by these sensors (Rehak et al., 2013). Therefore, research efforts are needed to mitigate the impact of using low-cost cameras on the quality of the reconstructed surfaces using the images acquired by these systems. So far, a few approaches have been proposed for 3D surface reconstruction using the images acquired by low-cost UAV systems. These approaches have been designed and implemented based on multi-image matching techniques using semi-global matching algorithms (Hirschmuller, 2008; Gehrke et al., 2012), patch-based methods (Furukawa and Ponce, 2010), or optimal flow algorithms(Pierrot-Deseilligny and Paparoditis, 2006). In these approaches, 3D surfaces are reconstructed using automated dense matching techniques and represented as dense 3D colored point clouds. However, these point clouds might not preserve edges or accurately represent the scanned surfaces due to point density variations. Moreover, these point clouds do not provide semantic information pertaining to individual scanned objects in those scenes. In order to overcome these drawbacks, a new region-based approach for 3D surface reconstruction using the images captured by cameras mounted on low-cost UAV systems is presented in this paper. This approach aims to generate a photorealistic 3D model from the individual scanned objects

* Corresponding author

using photogrammetric data processing and innovative texturing techniques. Figure 1 shows the outline of the proposed method for 3D surface reconstruction from the images collected by a digital camera/cameras mounted on UAS.

This paper starts by the introduction of the proposed method for 3D reconstruction of the scanned surfaces by cameras mounted on a UAS. Afterwards, experimental with real data are presented to verify the feasibility of the proposed approach. Finally, concluding remarks and recommendations for future research work are outlined.

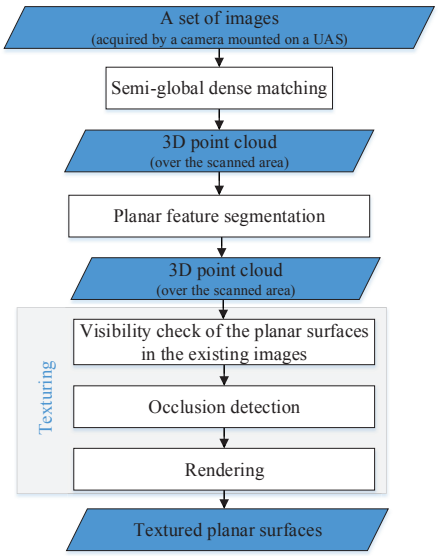

Figure 1. The outline of the proposed 3D surface reconstruction approach

2. METHODOLOGY

In this section, the proposed procedure for 3D surface reconstruction from the images collected by a camera/cameras mounted on a low-cost UAS is introduced. In the first step of this procedure, a Semi-Global dense Matching (SGM) algorithm is used to generate a 3D dense point cloud from the scanned scene using the captured images. The derived unstructured point cloud is generally sufficient for scene/terrain representation and visualization purposes. However, for the majority of aforementioned mapping and modelling applications, individually reconstructed surfaces are required. Therefore, in the next step of this procedure a parameter-domain segmentation approach is utilized to extract individual planar surfaces from the generated dense point cloud. Finally, a novel region-based texturing technique is implemented for photorealistic 3D reconstruction of the extracted planar surfaces. In the following subsections, the detailed explanation of these steps will be presented.

2.1 Dense Point Cloud Generation

In order to generate a dense point cloud from the area scanned within the captured images, a Semi-Global dense Matching (SGM) procedure is implemented. This procedure is initiated by the determination of camera's/cameras' exterior orientation parameters at each imaging station using a Structure from Motion (SfM) approach. Since the introduced dense matching approach has been mainly adopted for low-cost UAS which are not equipped with high-end Positioning and Orientation systems (POS), an initial recovery of the involved images' EOPS is required. In this paper, EOPs of the involved images are initially approximated using the approach proposed by He and Habib (2014). In the first step of this procedure, the conjugate points between stereo-pair images are identified using the Scale-Invariant Feature Transform (SIFT) algorithm. The EOPs of the involved images are then approximated in two steps: (1) the relative orientation parameters relating all possible stereo-images are derived from the essential matrix that is directly computed from conjugate point features, and (2) a local coordinate frame is established and incremental image augmentation process is performed to reference all the remaining images into a local coordinate frame. Since this approach is based on a linear solution for both relative orientation and initial approximation of image EOPs, it does not require any initial approximation for the optimization process. In addition, it can be applied in the absence of positioning/orientation information for the collected images.

In order to recover the EOPs of the captured images, conjugate points, which are identified from the aforementioned SIFT matching process, are then tracked through all images. The acquired images are normalized based on epipolar geometry – while considering camera IOPs and their estimated EOPs – to minimize the search space for tracking corresponding features in overlapping imagery. Finally, a dense 3D point cloud is generated based on a linear spatial intersection of light rays from all matched pixels.

2.2 Point Cloud Segmentation

In this paper, the parameter-domain segmentation approach proposed by (Lari and Habib, 2014) is utilized for the extraction of planar regions from the generated dense point cloud. In the first step of this segmentation procedure, a Principal Component Analysis (PCA) of local neighborhoods of individual points is performed to detect and model potential planar neighborhoods within the point cloud (Pauly et al., 2002). Afterwards, geometric attributes describing the detected planar neighnorhoods are estimated using an adaptive cylindrical buffer defined based on the PCA outcome (Figure 2). This cylindrical buffer is a modified version of adaptive cylinder neighborhood proposed by Filin and Pfeifer (2005). The diameter of this cylindrical buffer is specified by the distance between the query point and its n^{th}-nearest neighbor, where n is the number of points required for reliable plane definition while considering the possibility of having some outliers. The orientation of the cylinder axis is adaptively changing to be aligned along the normal to the plane through the majority of the neighboring points and the height of this cylindrical buffer – maximum normal distance between a neighboring point and best fitted plane – is usually determined based on the noise level in the point cloud coordinates.

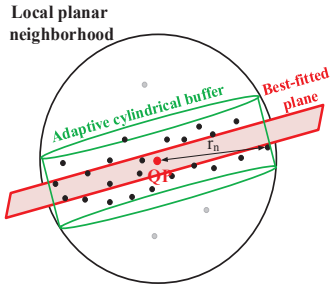

Figure 2. Adaptive cylindrical buffer of a query point (QP) belonging to a planar neighborhood

In order to speed up the segmentation process, the classification and representation of local planar neighborhoods is followed by a region growing procedure to aggregate all the points which belong to planar features into groups based on local point density variations. Further processing steps are carried out for the individual groups of planar surfaces rather than the entire points classified as being part of these surfaces. The segmentation attributes associated with the individual points, which belong to local planar neighborhoods, are then defined as the coordinates of the origin point's projection onto the best-fitted plane (X_0, Y_0, Z_0) to that planar neighborhood. Afterwards, a clustering approach is utilized for the detection and extraction of the accumulated peaks in the attribute space. In this segmentation approach, the estimated attributes are firstly organized in a kd-tree structure, which is manipulated for peak detection. A novel peak detection approach is then implemented, for which an appropriate extent of the cluster is estimated while considering acceptable angular and spatial deviation among the attributes of coplanar points. All the points in the parameter domain are checked to count the number of their neighboring points within the established cluster extent. The attribute point with the highest neighbors' count is chosen as the peak. The points in the spatial domain whose attributes are the constituents of the detected peak are then considered as one segment and removed from the parameter domain. The search for the highest count peaks is continued until the number of detected attribute points in the identified peak is less than the max number of the points within smallest region to be segmented. The disadvantage of such a segmentation procedure is that the points belonging to coplanar but spatially disconnected planes will be segmented into the same cluster. In order to resolve this ambiguity, a neighborhood analysis is conducted through boundary detection of the clustered points using the modified convex hull algorithm (Jarvis, 1977).

2.3 Region-based Texturing

In this subsection, a new approach for texturing individual segmented planar regions is introduced. This approach aims to provide a photo-realistic representation of the scanned surfaces within the captured images by camera/cameras mounted on UASs. The proposed texturing procedure is initiated by investigating the partial/full visibility of the segmented planar regions in the available imagery. Once the visibility of the segmented regions in the available imagery is checked, an occlusion detection procedure is performed to check if a planar region is occluding/being occluded by other regions in the field of view of existing images. In the next step, the segmented planar regions are decomposed based on their visibility within the available images. Finally, a rendering procedure is implemented to visualize the textured planar regions on the screen. The detailed explanation of these steps will be presented in the following subsections.

2.3.1 Visibility Check

In the first step of this texturing procedure, a visibility analysis technique is implemented to check if a segmented planar region is fully or partially visible in the available imagery. One should note that this procedure does not consider whether the region of interest is occluded by other regions in the field of view of a given image. In the proposed technique, the suitability of available images for the texturing of a planar region is initially investigated while considering the angle between the region surface normal and the optical axis of the image. For a given region, the image in question is considered to be appropriate for the texturing procedure if the region surface normal makes an acute angle with the optical axis of the image.

For the images which satisfy the abovementioned condition, the image footprint (the four corners of each image) is projected onto the infinite plane encompassing the planar region of interest using collinearity equations, while enforcing the plane equation of the region of interest. The overlap area between the projected image footprint and the planar region of interest is then identified to determine if the planar region is fully or partially visible within the image in question. The overlap area between two planar regions is identified using the Weiler-Atheron algorithm, which allows for intersecting a planar region by an arbitrarily-shaped polygon-window (Weiler and Atherton, 1977)

The planar region of interest is fully visible in an image if it is completely covered by the projected image footprint (Figure 3.a). On the other hand, the region of interest is partially visible in an image if more than the pre-specified percentage of the region area is covered by the projected image footprint (Figure 3.b). Once this visibility check is carried out for all planar regions in all images, a list of the appropriate images that could be used for the texturing of a given region is established.

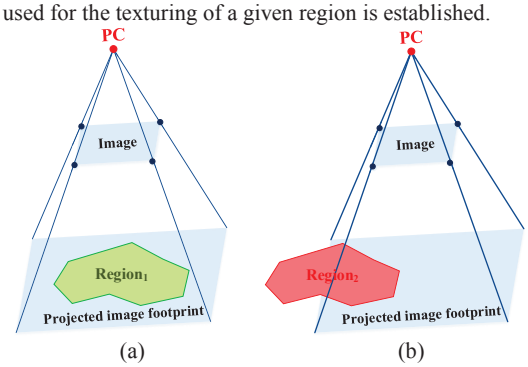

Figure 3. Representation of (a) a fully visible region and (b) a partially visible region in an image

2.3.2 Occlusion detection

In the previous step, the visibility of the planar regions in the images was checked without considering the possibility of them occluding/being occluded by the other planar regions. The objective of this step is to investigate whether the visible part of a planar region in an image is occluding/being occluded by the other regions in the field of view of that image. An option for conducting this test is to check whether or not every point in the overlap area between the region of interest and the footprint of the image in question is visible in that image. A point will be visible in a given image if the line of sight connecting the perspective center of the image to that point does not intersect any other region. A problem with this option is that we can derive an infinite number of points in the overlap area between a given region and the projected image onto that region. Therefore, the visibility analysis of these points in the given image will be time and memory consuming.

One way of overcoming this problem is to tessellate the overlapping area according to the sampling intervals of the individual pixels of a given image on the planar surface of the region of interest. This process will be quite memory expensive. Also, for regions that are not parallel to the plane of the image in question, there is no unique sampling distance. In order to avoid the aforementioned problems, an alternative occlusion detection approach will be adopted in this section. The conceptual basis of this alternative process is based on the boundaries (inner and outer boundaries) of the segmented

region as well as their intersection with the footprint of the image in question. This procedure is implemented by checking whether or not a boundary point is visible in a given image. This visibility analysis is performed by intersecting the line segment connecting the perspective center of a given image and the boundary point in question with all the regions that are visible in that image. If the intersection point is outside the investigated region, the boundary point is not occluding/ being occluded by that region within the image in question (Figure 4.a). Alternatively, if the intersection point happens to be inside the investigated region, the boundary point is either occluding or being occluded by the intersection point (Figure 4.b).

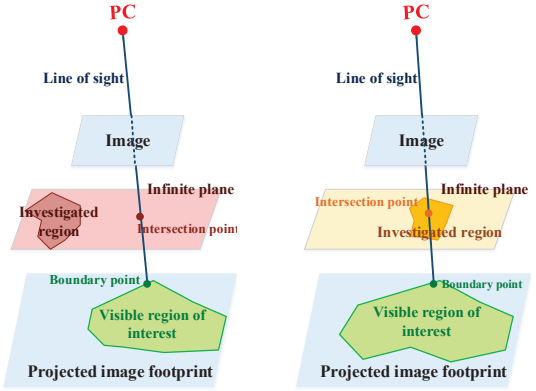

Figure 4. Visibility analysis of a planar region's boundary point in a given image, (a) intersection point outside of region boundary (b) intersection point inside region boundary

The boundary point will be occluded by the intersection point if the latter is closer to the perspective center than the former. On the other hand, the boundary point will be occluding the intersection point if the former is closer to the perspective center. In the first case, where the boundary point of the region of interest is occluded, the boundary points of the occluding region are projected onto the region of interest to determine the part of that region which is occluded in the given image. The occluded part is then identified by intersecting the planar region of interest with the projected occluding region onto the infinite plane of that region (Figure 5).

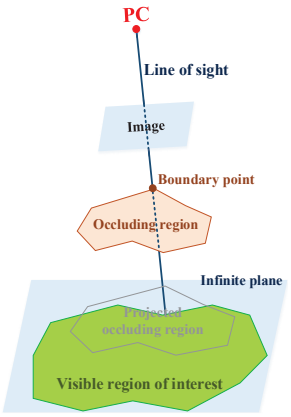

Figure 5. Identification of the occluded part of the region of interest (projection of boundary points of the occluding region onto the region of interest's infinite plane)

In the second case, where the region of interest is occluding another region, two different situations may occur:

1. All the boundary points of the region of interest are projected inside the occluded region (Figure 6(a)).
2. A portion of the boundary points of the region of interest are projected inside the occluded region (Figure 6(b)).

The first situation can be solved by projecting the boundary points of the region of interest onto the occluded region. Once the boundary points of the region of interest are projected onto the occluded region, the occluded part within that region is determined and subtracted to identify the visible part of that region in the given image. The second situation will be handled when the occluded region becomes the region of interest. For each of the visible regions in an image, one can sequentially trace the visible boundary points, the points along the image footprint intersection with the region, if they happen to be inside the region, and the internal points that are occluded by the boundary points of the other regions. The outcome of this procedure, for a given region, will be the sub-regions that are visible in different images.

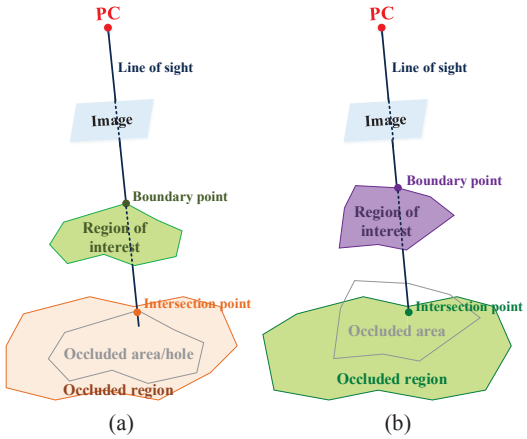

Figure 6. The occlusion of other regions by the region of interest (a) all the boundary points of the region of interest are projected inside the occluded region and (b) a section of the boundary points are projected inside the occluded region

2.3.3 Decomposition of segmented planar regions

Once the visible part/parts of the planar regions within available images are identified through the proposed procedures in the previous two subsections, the segments of these parts which will be textured using the individual images should be identified. In this section, a decomposition approach is introduced to determine these segments within individual planar regions. In other words, the objective of this procedure is to identify which parts of each planar region will be textured as best as possible using individual images. In this case, we are dealing with one of the following three scenarios:

1. The first scenario deals with planar regions which are entirely visible in a single or multiple images. If this region is visible in a single image, all of its boundary points are projected onto that image and the part of the image within the projected boundary will be rendered onto the given region. On the other hand, if a given region is fully visible in multiple images, its texturing procedure is carried out using the image that has the best homogenous sampling distance along that region. The image which has the best homogenous sampling distance is defined as the image which is closest to the region of interest and has the smallest angle between the surface normal and the optical axis of the image.

1. The second scenario deals with the regions which are partially visible in multiple images (Figure 7). The texturing of these regions is carried out by decomposing the visible sub-regions into the parts which are visible in single or multiple images. In order to identify these parts, the visible sub-regions in the individual images first are intersected together using the Weiler-Atheron algorithm. One should note that the occluded parts of the visible sub-regions in each image were identified in the previous step. Figure 8 shows the visible sub-regions in each image and Figure 9 shows the outcome of intersecting these sub-regions. The intersected parts of the visible sub-regions represent the segments which are visible in multiple images ($segment_{12}$ and $segment_{23}$). The overlap areas between the sub-regions (i.e., the segments that are visible in multiple images) are then subtracted from the individual sub-regions to identify the segments which are visible in a single image (i.e., $segment_{11}$, $segment_{22}$, and $segment_{23}$).

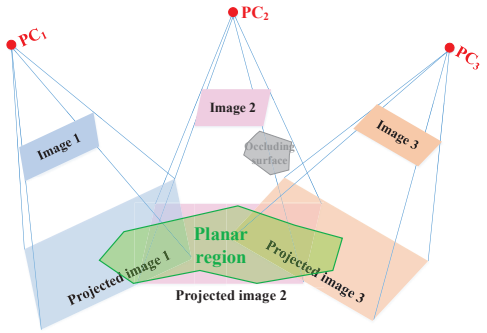

Figure 7. A planar region which is partially visible in the overlapping images

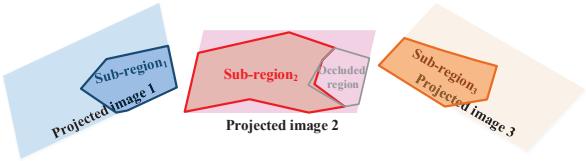

Figure 8. Visible sub-regions of the planar region in the overlapping images

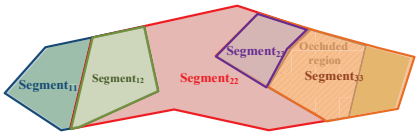

Figure 9. The intersection between visible sub-regions in each image

For the segments which are visible in a single image, the rendering procedure is carried out by projecting their boundary points onto that image and selecting the part of the image within the projected boundary for texturing that segment (Figure 10). However, for the segments which are visible in multiple images, the rendering procedure is carried out using all the images encompassing those segments. Accordingly, the boundary points of such a segment are projected onto all of the images enclosing that segment. The assigned color to a pixel within the master texture is determined by averaging the colors of its conjugate pixels in all images enclosing the projected boundary in question. The intersected segment then will be textured using the established master texture (Figure 11).

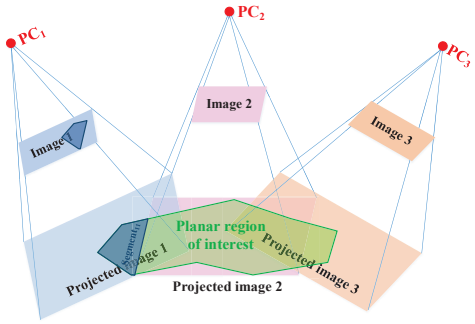

Figure 10. Rendering a segment which is visible in a single image ($segment_{11}$)

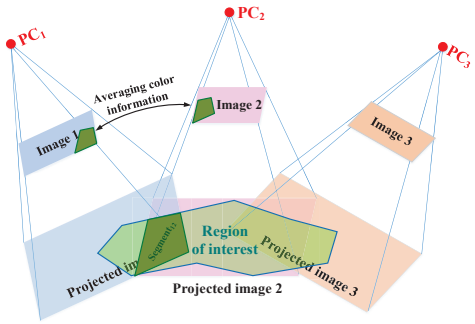

Figure 11. Rendering a segment which is visible in two images

2.3.4 Rendering and visualization

Once the parts of planar regions are decomposed according to their visibility within individual images, a rendering procedure should be implemented to render and visualize them on the screen. The objective of this procedure is to apply the identified textures, within the images, to the segmented planar surface in 3D space and visualize the textured surfaces on the 2D screen. More specifically, in rendering procedure, the clipped textures are rendered onto the segmented planar surface in 3D object space, which is then mapped to the destination image (on the screen) using projective transformation.

In this texturing procedure, the transformation between object space and texture space was already established using the collinearity equations in the previous section while the transformation between the object space and screen is carried out using the Open Graphics Library (OpenGL) programming interface (Shreiner, 2009). In order to optimize the performance of the rendering procedure, OpenGL is only able to render convex and solid planar surfaces onto 2D screen space. However, in reality, we are also dealing with concave planar surfaces, planar surfaces with holes, and complex planar surfaces. In order to handle the projection of theses surfaces onto a 2D screen, they should be tessellated into simple convex polygons. Therefore, the Delaunay triangulation algorithm (Bowyer, 1981; Watson, 1981) is utilized to subdivide concave, hollow, and complex polygons into easier-to-render convex polygons (triangles). Since the correspondence between texture space and object space has already been established through the texturing procedure, the vertices of the derived triangles, in the object space, are identified on the assigned texture to the planar region of interest to determine the parts of the texture that belongs to those triangles. The clipped textures are then rendered onto the triangles and visualized in 2D screen space. One should note that the identified textures and the objects to

be textured, on the screen, are rarely the same size in pixels. Therefore, filtering techniques should be applied to determine how each pixel, in the original texture image, should be expanded or shrunk to match a screen pixel size.

3. EXPERIMENTAL RESULTS

In order to verify the feasibility of the proposed approach for the 3D reconstruction of individual surfaces scanned by a camera/cameras mounted on unmanned aerial systems, experiments using the real data are conducted and presented in this section. The utilized dataset for this experiment for this experiment includes 28 images acquired over a complex building using a GoPro HERO3 camera mounted on a low-cost UAS (DJI Phantom 2) at an average flying height of 26m. Table 1 summarizes the specifications of the images collected over the building of interest. Figures 12.a and 12.b show an overview of the area of interest as seen from Google Earth and the SGM-generated point cloud (displayed in different colors according to the height), respectively.

Table 1. A summary of Ronald MacDonald's house photogrammetric dataset characteristics

Dataset	Photogrammetric data
System	GoPro HERO 3+ black edition
Date acquired	2014
Number of images	28
Ground sampling distance	1.7 cm
Planimetric accuracy	1.7 cm
Vertical accuracy	6 cm

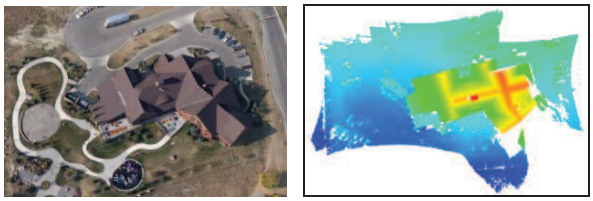

(a) (b)

Figure 12. (a) An overview of the building of interest from Google Earth and (b) SGM-generated point cloud colored according to height over same area (c)

The generated 3D point cloud is initially segmented to establish the individual planar surfaces. The extracted planar surfaces are then textured using the proposed surface reconstruction approach to create a photorealistic 3D model of the scanned area. Figures 13 and 14 show the extracted planar features from the generated 3D point and two different views of the reconstructed photorealistic 3D model, respectively.

Figure 13. Segmented point cloud (extracted planar surfaces) over the area of interest

(a)

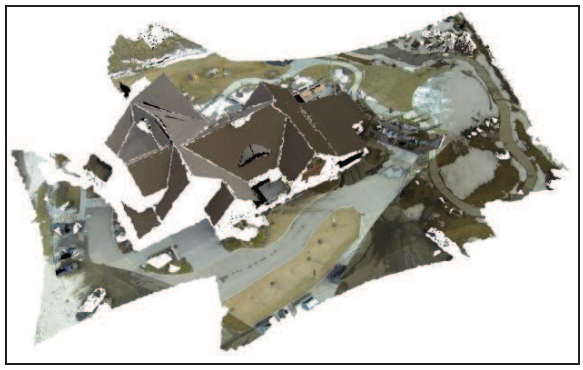

(b)

Figure 14. Two different views from the reconstructed planar regions

Qualitative evaluation of the derived results through visual inspection of Figures 14.a and 14.b verified the feasibility of the proposed approach for photorealistic 3D surface reconstruction using overlapping images collected by a camera mounted on a UAS.

4. CONCLUSIONS AND RECOMMENDATIONS FOR FUTURE RESEARCH WORK

This paper introduced a new approach for photorealistic 3D surface reconstruction using the images acquired by a camera/cameras mounted on low-cost UAS. This approach is implemented in three steps: in the first step, a SGM technique is utilized to generate a 3D point cloud from the scanned scene within the captured images. The contribution of the implemented dense matching approach is linear recovery of EOPs of the involved images without the need for initial approximations. In the second step, the generated 3D point cloud is segmented using a parameter-domain approach to extract individual planar features scanned within the acquired images. In the third step, a new texturing technique is implemented for photorealistic reconstruction of the extracted planar surfaces. This texturing procedure starts by investigating the full/partial visibility of the individual extracted surfaces within the acquired images. A novel occlusion detection procedure is then carried out to check whether visible part/parts of a planar surface in an image is occluding/being occluded by the other extracted surfaces in the field of view of that image. This procedure is implemented by checking whether the boundary points of an extracted planar surface are visible in a given image or not. Afterwards, a surface decomposition procedure is performed to determine which part/parts of each planar surface will be textured as best as possible using individual images. A rendering procedure is finally implemented to apply the identified textures within the images to the segmented planar surfaces in 3D space and visualize the textured surfaces on the 2D screen.

Qualitative evaluation of the derived outcome verified the feasibility of the proposed approach for 3D surface reconstruction using the images captured by camera/cameras mounted on a low-cost UAS. In conclusion, the introduced procedure resolves the shortcomings of previously-developed surface reconstruction approaches provides a photo-realistic view of individual scanned surfaces. The reconstructed 3D surfaces can be ultimately utilized for different surface interpretation, object extraction, modelling, and monitoring

applications. Future research work will be focused on the extension of the proposed approach for 3D reconstruction of non-planar surfaces (e.g., linear/cylindrical features, cones, spheres) to provide complete view of the scanned scenes. In addition, the assigned textures to the segmented planar regions can be processed using image processing techniques (e.g., image segmentation) to identify and quantify characteristics of individual planar features (e.g., possible deteriorations or cracks that have not been properly represented in the laser scanning point cloud).

ACKNOWLEDGEMENTS

The authors would like to thank the Natural Sciences and Engineering Research Council of Canada Strategic Project Grants (NSERC SPG) for financial support of this research work.

REFERENCES

Bowyer, A., 1981. Computing Dirichlet tessellations. *Comput. J.* 24, 162–166.

Eisenbeiss, H., 2011. The potential of Unmanned Aerial Vehicles for mapping. *Presented at the Photogrammetric Week 2011*, pp. 135–145.

El-Sheimy, N., 2005. An overview of mobile mapping systems, in: From Pharaohs to Geominformatics. *Presented at the FIG Working Week 2005 and GSDI-8*, Cairo, Egypt, pp. 1–24.

Everaerts, J., 2008. The use of unmanned aerial vehicles (UAVs) for remote sensing and mapping., in: *The International Archives of the Photogrammetry, Remote Sensing and Spatial Information Sciences*. pp. 1187–1192.

Filin, S., Pfeifer, N., 2005. Neighborhood systems for airborne laser data. *Photogramm. Eng. Remote Sens*. 71, 743–755.

Furukawa, Y., Ponce, J., 2010. Accurate, dense, and robust multiview stereopsis. *IEEE Trans. Pattern Anal. Mach. Intell.* 32, 1362–1376.

Gehrke, S., Downey, M., Uebbing, R., Welter, J., LaRocque, W., 2012. A multi-sensor approach to semi-global matching. in: *The International Archives of the Photogrammetry, Remote Sensing and Spatial Information Sciences*. Vol. XXXIX-B3, pp. 17–22.

He, F., Habib, A., 2014. Linear approach for initial recovery of the exterior orientation parameters of randomly captured images by low-cost mobile mapping systems, in: *The International Archives of the Photogrammetry, Remote Sensing and Spatial Information Sciences*. Vol XL-1, pp. 149–154.

Hirschmuller, H., 2008. Stereo processing by semiglobal matching and mutual information. *IEEE Trans. Pattern Anal. Mach. Intell.* 30, 328–341.

Lari, Z., Habib, A., 2014. An adaptive approach for the segmentation and extraction of planar and linear/cylindrical features from laser scanning data. *ISPRS J. Photogramm. Remote Sens*. 93, 192–212.

Nagai, M., Chen, T., Shibasaki, R., Kumagai, H., Ahmed, A., 2009. UAV-borne 3-D mapping system by multisensor integration. *IEEE Trans. Geosci. Remote Sens.* 47, 701–708.

Pauly, M., Gross, M., Kobbelt, L.P., 2002. Efficient simplification of point-sampled surfaces, in: *Proceedings of the Conference on Visualization (VIS) 2002. IEEE Computer Society*, Washington, DC, USA, pp. 163–170.

Pierrot-Deseilligny, M., Paparoditis, N., 2006. A multiresolution and optimization-based image matching approach: an application to surface reconstruction from SPOT5-HRS stereo imagery, in: *The International Archives of the Photogrammetry, Remote Sensing and Spatial Information Sciences*.. Vol. 36 (I/W41).

Rehak, M., Mabillard, R., Skaloud, J., 2013. A micro-UAV with the capability of direct georeferencing. in: *The International Archives of the Photogrammetry, Remote Sensing and Spatial Information Sciences*. Vol. XL-1/W2, pp. 317–323.

Shreiner, D., 2009. OpenGL Programming Guide: The Official Guide to Learning OpenGL, Versions 3.0 and 3.1 (7th Edition). Addison-Wesley Professional, Indianapolis, IN, USA.

Tao, C.V., Li, J., 2007. Advances in Mobile Mapping Technology. CRC Press.

Watson, D.F., 1981. Computing the n-dimensional Delaunay tessellation with application to Voronoi polytopes. *Comput. J.* 24, 167–172. doi:10.1093/comjnl/24.2.167

Weiler, K., Atherton, P., 1977. Hidden surface removal using polygon area sorting, in: *Proceedings of the 4th Annual Conference on Computer Graphics and Interactive Techniques, SIGGRAPH '77. ACM*, New York, NY, USA, pp. 214–222.